

THE STAR-FORMING REGION NGC 346 IN THE SMALL MAGELLANIC CLOUD WITH HUBBLE SPACE TELESCOPE ACS OBSERVATIONS I. PHOTOMETRY¹

D. A. GOULIERMIS², A. E. DOLPHIN³, W. BRANDNER², TH. HENNING²

Accepted for publication in The Astrophysical Journal Supplement Series, 22 June 2006

ABSTRACT

We present a photometric study of the star-forming region NGC 346 and its surrounding field in the Small Magellanic Cloud, using data taken with the Advanced Camera for Surveys (ACS) on board the Hubble Space Telescope (HST). The data set contains both short and long exposures for increased dynamic range, and photometry was performed using the ACS module of the stellar photometry package DOLPHOT. We detected almost 100,000 stars over a magnitude range of $V \sim 11$ to $V \sim 28$ mag, including all stellar types from the most massive young stars to faint lower main sequence and pre-main sequence stars. We find that this region, which is characterized by a plethora of stellar systems and interesting objects, is an outstanding example of mixed stellar populations. We take into account different features of the color-magnitude diagram of all the detected stars to distinguish the two dominant stellar systems: The stellar association NGC 346 and the old spherical star cluster BS 90. These observations provide a complete stellar sample of a field about $5' \times 5'$ around the most active star-forming region in this galaxy. Considering the importance of these data for various investigations in the area, we provide the full stellar catalog from our photometry. This paper is the first part of an ongoing study to investigate in detail the two dominant stellar systems in the area and their surrounding field.

Subject headings: Magellanic Clouds — Color-Magnitude diagram — stars: evolution — techniques: photometric — clusters: individual (NGC 346, [BS95] 90) — catalogs

1. INTRODUCTION

The investigation we present here deals with the stellar content of the star forming region in the vicinity of the stellar association NGC 346 in the Small Magellanic Cloud (SMC). NGC 346 is the largest stellar concentration in the SMC, related to the brightest HII region of this galaxy, named LHA 115-N 66 or in short N 66 (Henize 1956), with an $H\alpha$ luminosity almost 60 times higher than Orion's (Kennicutt 1984). Such active star forming regions are rare and can only be compared to star-bursts, like e.g., NGC 3603 in our Galaxy (Sher 1964). As a consequence NGC 346 has been the subject of intense studies to establish the properties of the HII region and of the bright early-type stellar content of the association in the low-metallicity environment of the SMC.

In a spectroscopic study of 42 bright main sequence stars Massey et al. (1989) confirmed 33 O-stars in the area of NGC 346. 22 of them are located in the central region of the association, and eleven are of type O6.5 or earlier. The stellar sample of Massey et al. is essentially complete down to $\sim 10 M_{\odot}$ with six stars in the mass range 40 - 85 M_{\odot} and with a background field population of $\sim 5 M_{\odot}$ stars.

An ultraviolet and optical spectral atlas of O stars in the SMC is compiled by Walborn et al. (2000) with data from the HST Space Telescope Imaging Spectrograph (STIS), AAT and ESO 3.6 m. Systematic phenomena in the sample include weak stellar-wind profiles on the O main sequence and in late-O giants, the absence of Si IV wind features throughout the O-giant sequence, low terminal velocities and enhanced He II wind features in Of super-giants. The spectra of six O-type stars in NGC 346 from the Walborn et al. (2000) sample were

modeled by Bouret et al. (2003) to determine their chemical abundances and wind parameters. The majority of the stars reveal CNO cycle-processed material at their surfaces during the main-sequence stage, thus indicating fast stellar rotation and/or very efficient mixing processes. The derived effective temperatures are lower than predicted from the widely used relation between spectral type and T_{eff} , resulting in lower stellar luminosities and lower ionizing fluxes.

However, Massey et al. (2005) argue that the data used by Bouret et al. (2003) were limited with respect to sky (nebular) subtraction. The effective temperatures of O3 - O7 dwarfs and giants in the SMC, as found by Massey et al. (2005) from their investigation of 33 O-type stars in the Magellanic Clouds, are about 4000 K hotter than for stars of the same spectral type in the Milky Way. Consequently, the effective temperature scale for O dwarfs in NGC 346 derived by these authors is significantly hotter than the Bouret et al. (2003) values. The differences decrease as one approaches stars of spectral type B0 V. In general, Massey et al. (2005) found that the winds momentum of O stars in the Magellanic Clouds scales with luminosity and metallicity as predicted by the theory for radiatively driven wind (Kudritzki 2002; Vink et al. 2001), supporting the use of photospheric analyses of hot luminous stars as a distance indicator for galaxies with resolved massive stellar populations.

A search for Be-stars in a field of $10' \times 10'$ centered on NGC 346 (Keller et al. 1999) found that only about 11% of the upper main sequence stars (with $V < 16$ mag) located in the main body of the association show indeed strong $H\alpha$ emission. These authors adopt the most widely accepted explanation for the Be phenomenon, the rapid rotation of the B star (Bjorkman & Cassinelli 1993), due to which the stellar wind from a star is concentrated and confined to a disk around its equatorial plane. They relate, thus, the low fraction of Be stars in the cluster with the suggestion that it has been formed from low angular momentum gas.

The general area of NGC 346/N 66 hosts at least two super-

¹ Research supported by the Deutsche Forschungsgemeinschaft (German Research Foundation)

² Max-Planck-Institut für Astronomie, Königstuhl 17, D-69117 Heidelberg, Germany, dgoulie@mpia.de, brandner@mpia.de, henning@mpia.de

³ Steward Observatory, 933 N. Cherry Avenue Tucson, AZ 85721-0065, USA, adolphin@as.arizona.edu

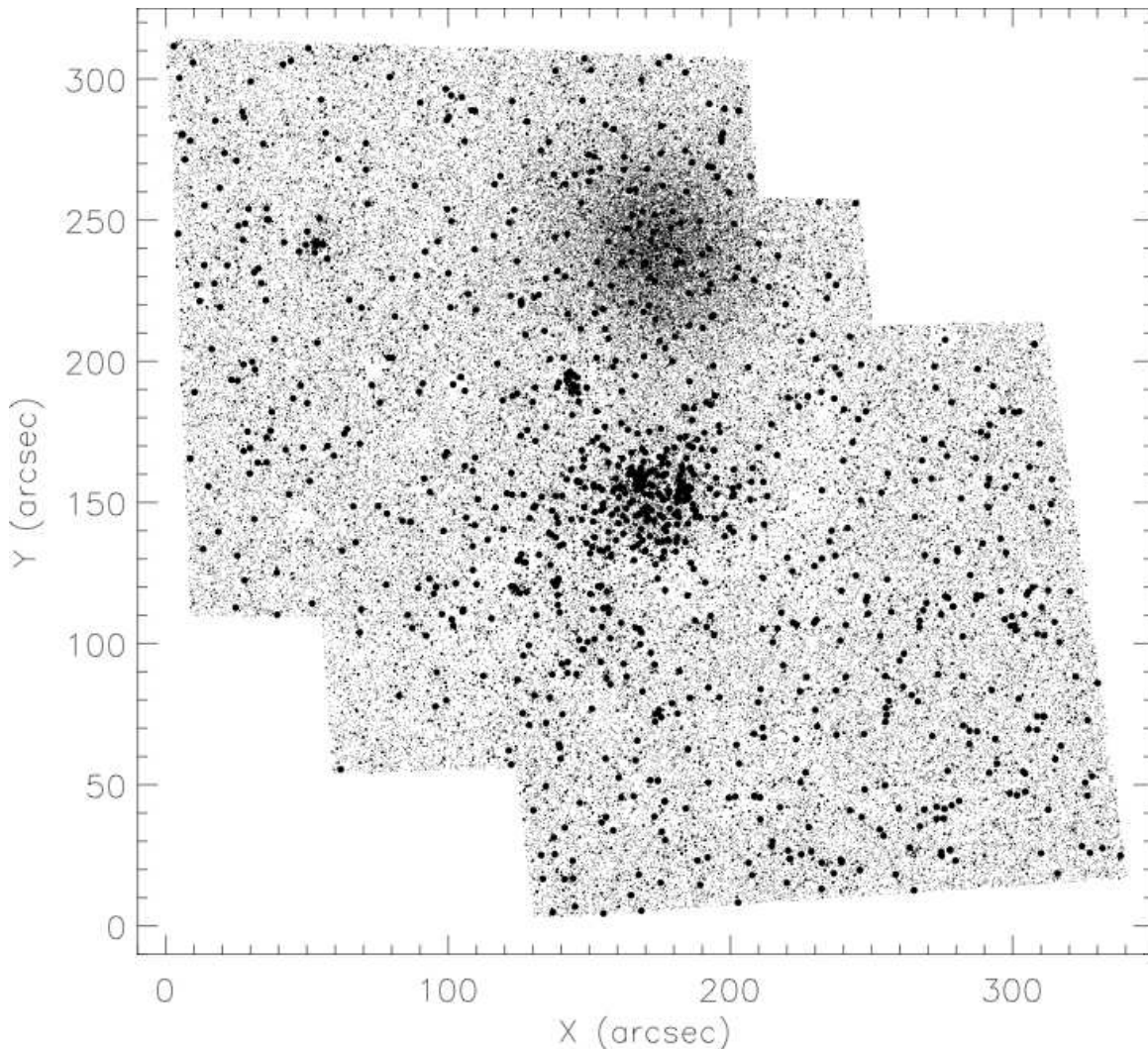


FIG. 1.— Map of stars found in both F555W and F814W filters with DOLPHOT photometry based on ACS/WFC imaging of three fields. The map covers the whole area around the association NGC 346 in the SMC. North is up and east is left. Coordinates refer to the drizzled F814W image and are given in seconds of arc.

nova remnants. Not much is known about the first, named SNR 0056–7233, which has been identified by Ye et al. (1991) to the southwest at a projected distance of about 5.4 pc from the center of NGC 346. The second supernova remnant, named SNR 0057–7226, is located northeast close to the Wolf-Rayet luminous blue variable system HD 5980 in the vicinity of NGC 346. Koenigsberger et al. (2001) observed with HST/STIS interstellar and circumstellar absorption components along the line of sight toward HD 5980. They argued that SNR 0057–7226 had probably a progenitor, that was one of the brightest members of the association. An estimation of $T \sim 40,000$ K and a total mass between 400 and 1000 M_{\odot} for the supernova remnant shell was made by these authors. *Chandra* observations have shown that HD 5980 is surrounded by a region of diffuse X-ray emission from the supernova remnant, while NGC 346 itself shows only relatively faint X-ray emission, most of which seems correlated with the location of the brightest stars in the core of the association (Nazé et al. 2003).

Danforth et al. (2003) found with the *Far Ultraviolet Spectroscopic Explorer* (FUSE) strong O VI and C III emission from a position at the edge of SNR 0057–7226. They de-

termined the physical parameters of the interaction zone with N 66 and found that ionizing photons from massive stars of the association likely affect the ionization balance in the post-shock gas, hindering the production of lower ionization and neutral species. Danforth et al. (2003) proposed a physical relationship between SNR 0057–7226 and N 66, which suggests a slowly expanding bubble around NGC 346, powered by stellar winds and thermal pressure, while strong O VI, C III, and X-ray emission arise from the shock interaction of the supernova remnant with the denser, ionized gas on the rear side of N 66.

Relaño et al. (2002) computed photoionization models of the H II region around NGC 346 with the CLOUDY 94 algorithm (Ferland et al. 1998) based on spectrophotometric data of Peimbert et al. (2000). These models showed that about 45% of the photons produced by the ionizing stars escape from NGC 346, implying that the system is a major source of ionizing flux for the surrounding diffuse interstellar medium. They also suggested that N 66 is a spherical density-bounded nebula.

The recent release of the *Advanced Camera for Surveys* imaging toward the general area of NGC 346 from the *HST*

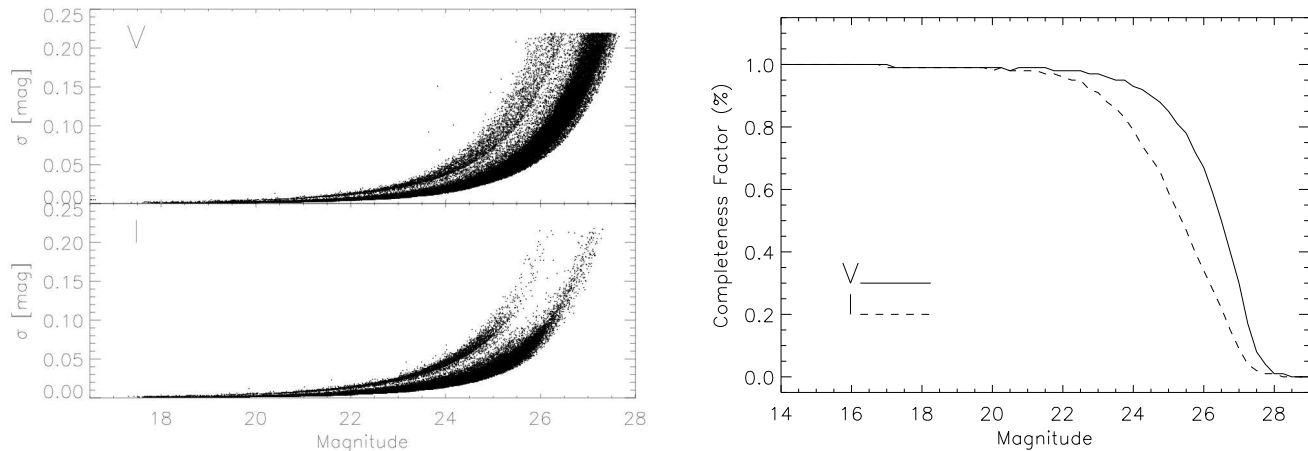


FIG. 2.— Typical uncertainties of photometry (left) and completeness factors (right) as derived by DOLPHOT from all datasets, for both bands. The bifurcation in the photometric errors is due to varying depth within the overall field. The stars in the high-sigma branch are located in regions covered only by single exposures (dataset J92FA3).

Data Archive offers a unique opportunity for the detailed photometric study not only of the bright massive stellar content, which is well known, but mostly of the fainter stellar members of the area down to the lower main sequence stars, which represent the majority of the stellar populations. In this paper we present our photometry of these observations, that cover a field about $5' \times 5'$ centered on the association NGC 346. Our photometry detects magnitudes as faint as $V \gtrsim 26.5$ mag, providing one of the richest stellar samples observed in the SMC. We also describe the stellar content of the area as it is seen in the derived color-magnitude diagram.

Specifically, in section 2 we present the observations and the photometry with software especially designed for ACS imaging. In the following section we present the stellar catalog and the color-magnitude diagram. We identify the different stellar populations coexisting in the area and we discuss their spatial distribution (§3). A general description of the stellar content of the two main stellar concentrations in the area, the young stellar association NGC 346, and the old spherical cluster [BS95] 90 or in short BS 90 (Bica & Schmitt 1995) is given in section 4. Final remarks and future prospects of the science that this catalog can provide are discussed in section 5.

2. OBSERVATIONS AND PHOTOMETRY

The data were collected within the HST GO Program 10248 (PI A. Nota). Three pointings (with significant offsets) within a single field centered on the association NGC 346 were observed with the Wide-Field Channel (WFC) of ACS in the filters F555W and F814W, which are equivalent to standard V and I bands respectively. We obtained the data from the HST Data Archive. A detailed description of the datasets can be found in Table 1. The first visit (J92F01) covers the north-western part of the observed region, while the second visit (J92F02) covers the southeastern part. Each visit consists of long F555W and F814W exposures taken in a 4-point dither pattern, plus two short exposures in each filter at one pointing. There is also a third, central visit (J92FA3), which includes a single exposure in each filter (as well as $H\alpha$ and HRC images, which we are not using). The whole set of data provides a unique collection of deep observations toward the SMC. In addition, the short exposures complement the stellar sample

TABLE 1
LOG OF THE OBSERVATIONS. DATASETS REFER TO HST ARCHIVE CATALOG. EXPOSURE TIMES (T_{expo}) PER FILTER ARE GIVEN IN SECONDS.

Visit Dataset	RA	DEC (J2000)	T_{expo}	
			F555W	F814W
J92F01	00:59:07.61	-72:09:39.8	1×456	1×484
	00:59:07.31	-72:09:40.0	1×456	1×484
	00:59:07.02	-72:09:40.1	1×456	1×484
	00:59:06.72	-72:09:40.3	1×456	1×484
	00:59:06.72	-72:09:40.3	2×3	2×2
J92F02	00:59:05.58	-72:11:21.5	1×483	1×450
	00:59:05.28	-72:11:21.6	1×483	1×450
	00:59:04.99	-72:11:21.6	1×483	1×450
	00:59:04.68	-72:11:21.7	1×483	1×450
	00:59:04.68	-72:11:21.7	2×3	2×2
J92FA3	00:59:06.18	-72:10:31.2	1×380	1×380

with the more massive stars of the area, which occupy both the main sequence and the red giant branch as it will be shown later.

We obtained the pipeline-reduced FITS files from the HST Data Archive. In order to clean the images of residual warm pixels and cosmic rays, we ran *multidrizzle* (Koekemoer et al. 2002) using the recommended recipe for multiple visits from the ACS data handbook. The process involved first obtaining separately drizzled images, measuring the alignment offsets, and then creating the final drizzled image. Although we avoid photometry on drizzled frames whenever possible (due to position-dependent smoothing and PSF blurring), the drizzling process is useful for generating a deep reference image of the entire field, and finding cosmic rays and bad pixels in the original images.

Photometry was obtained using the ACS module of the package DOLPHOT (version 1.0; Dolphin, in preparation). The short images could not be combined in the drizzle process in an easy way. These images were cleaned by the *imcombine* task of DOLPHOT. This was possible because the short images were taken in pairs with identical pointings, and thus the CRREJ-like cleaning algorithm was sufficient to re-

TABLE 2
 SAMPLE FROM THE PHOTOMETRIC CATALOG OF STARS FOUND IN THIS
 STUDY IN THE REGION OF NGC 346 WITH HST/ACS IMAGING.
 MAGNITUDES ARE GIVEN IN THE VEGA SYSTEM.

Star No.	RA (J2000)	DEC (J2000)	V (mag)	σ_V	I (mag)	σ_I
1	00:58:42.42	-72:09:43.02	12.171	0.001	11.491	0.001
2	00:59:04.46	-72:10:24.49	12.443	0.001	12.705	0.001
3	00:58:53.89	-72:12:04.50	13.526	0.002	11.887	0.001
4	00:58:36.09	-72:11:13.31	13.783	0.002	12.080	0.001
5	00:59:00.72	-72:10:27.91	13.519	0.001	13.750	0.002
6	00:59:00.01	-72:10:37.67	13.692	0.001	13.923	0.002
7	00:59:36.51	-72:10:22.33	14.382	0.003	14.386	0.004
8	00:58:36.18	-72:12:16.56	14.503	0.003	12.958	0.002
9	00:58:57.36	-72:10:33.38	13.977	0.002	14.193	0.002
10	00:59:01.77	-72:10:30.94	14.375	0.002	14.466	0.004
11	00:59:30.34	-72:09:09.40	14.578	0.003	14.721	0.004
12	00:59:41.39	-72:08:10.14	14.633	0.003	14.760	0.004
13	00:59:06.71	-72:10:41.02	14.654	0.002	14.812	0.003
14	00:59:06.31	-72:09:55.84	14.374	0.002	14.365	0.003
15	00:59:02.88	-72:10:34.68	14.448	0.002	14.700	0.003

move image defects. All 22 exposures were photometered simultaneously, using the F814W drizzled frame as the position reference. All photometry parameters were set equal to the recommended values in the DOLPHOT manual⁴. Photometric calibrations and transformations were made according to Sirianni et al. (2005), and CTE corrections were made according to ACS ISR 04-06.

In total we had 149,253 detections with $S/N \geq 5$ in both filters and object classifications as stellar. To clean bad detections from our photometric catalog, we applied two cuts using DOLPHOT's star quality parameters. First, to avoid residuals near bright stars, we eliminated all detections with a mean crowding parameter of 0.75 or higher (those objects that would be measured twice as bright if nearby stars were not subtracted). Second, to eliminate other non-stellar features, we eliminated all objects whose mean sharpness was less than -0.15 (generally cosmic rays) or greater than 0.15 (extended sources). After this procedure more than 99,000 stars were detected with our photometry (Figure 1). The full length of the photometric catalog with the X, Y positions and the V- and I-equivalent magnitudes (in the Vega system) of these stars is available in electronic form. Figure 2 (left panel) shows typical uncertainties of photometry as a function of the magnitude for both filters. The completeness of the data was evaluated by artificial star experiments, that were performed by running DOLPHOT in artificial star mode with the use of artificial star lists created with the utility *acsfakelist* of the ACS module for DOLPHOT. The completeness is found to be spatially variable, depending on the crowding of each region. The completeness functions for the whole observed field are shown in Figure 2 (right panel) for both filters.

3. STELLAR POPULATIONS

3.1. The Color-Magnitude Diagram

The region of NGC 346 is found to provide an excellent example of well resolved extra-galactic stellar populations. The $V-I$, V Color-Magnitude Diagram (CMD) of the detected stars (Figure 3) shows that the region is characterized by the

⁴ DOLPHOT, including the ACS module and documentation, can be found at the web-site <http://purcell.as.arizona.edu/dolphot/>

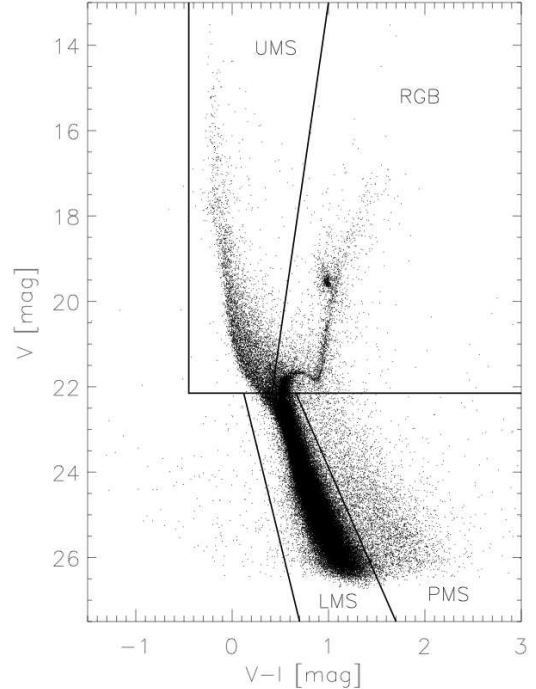


FIG. 3.— $V-I$, V Color-Magnitude Diagram (CMD) of all stars detected with the best photometry (see text) in the area of NGC 346 with ACS/WFC imaging. The limits of four regions, indicative of specific stellar populations, are overplotted. These regions represent the upper main sequence (UMS), the lower main sequence (LMS), the red giant branch (RGB) and the region where candidate pre-main sequence (PMS) stars have been previously identified.

coexistence of several stellar populations. There is a sharp upper main sequence (UMS) of young blue massive stars, a clear turn-off at around $V \simeq 22$ mag and a prominent red giant branch (RGB) with its red clump clearly located at around $V \simeq 19$ mag and $V-I \simeq 1.0$ mag. Below the turn-off the main sequence is becoming highly populated with what should be considered to be a well mixed collection of low-mass stars of several ages. Under this assumption, the lower main sequence (LMS) represents stars, which are located in one region of the CMD, but they could have been born during completely different star formation events. To the right of LMS and toward redder colors we find a concentration of low-mass stars, that do not fit to any classical scheme of stellar populations. Most likely they are pre-main sequence (PMS) stars.

Such stars have been found to exist in stellar associations of the Magellanic Clouds. Gouliermis et al. (2006) presented recently the case of the association LH 52 in the Large Magellanic Cloud, where they identified the candidate PMS population of the system with HST/WFPC2 observations in V and I . The detected PMS stars of LH 52 have the same location on the $V-I$, V CMD with the faint red sequence we observe in the CMD of Figure 3 to the right of the LMS. As far as the association NGC 346 is concerned, Brandner et al. (1999) already reported the detection of about 150 objects with excess emission in $H\alpha$ in a $2' \times 2'$ field slightly off the brightest stars of the association. They explained this detection as an indication that NGC 346 hosts PMS stars with masses between 1 and $2 M_{\odot}$. More recently, Nota et al. (2006) used their observations of NGC 346, taken within Visit J92FA3 (see table 1)

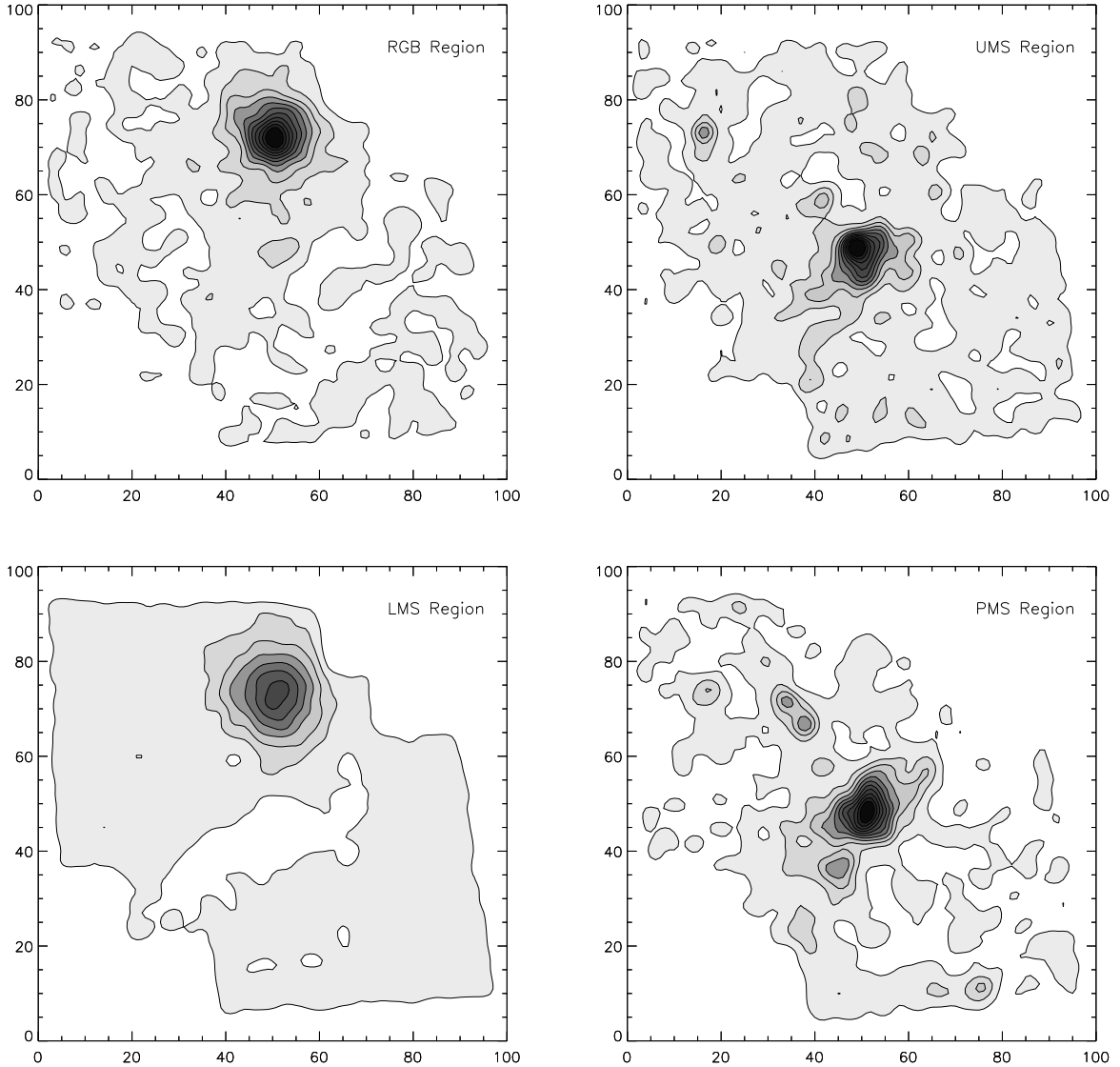


FIG. 4.— Isodensity contour maps constructed with star counts of four different stellar populations, which cover different regions in the CMD of Figure 3 (RGB, UMS, LMS, and PMS).

in filters F555W (V), F814W (I) and F658N ($H\alpha$), and they verified that there is a prominent population of candidate PMS stars located in this part of the CMD, “that have likely formed together with NGC 346 about 3-5 Myr ago”.

In order to make a first-order characterization of the observed stellar species we select four regions in the CMD, where each corresponds to one of the most prominent observed CMD features (UMS, LMS, RGB and PMS). The limits of the selected CMD regions are shown in Figure 3. We distinguish, thus, four selected stellar groups, and we plot the spatial distribution of each one with the use of star counts.

3.2. Characterization of the Observed Stellar Populations

We identify the area in the observed region where each type of stars is dominant by performing star counts, and we construct the spatial density distribution of each stellar kind. We use the photometric catalog of the detected stars to perform star counts on square grids, under the assumption that each

star is a point determined by its coordinates in the catalog. Each grid element has dimensions $\simeq 70$ WFC pixels, or $\simeq 3''5$, which corresponds to about 1 pc at the distance of the SMC of about 60 kpc (Dolphin et al. 2001). This star count algorithm is originally used for the detection of stellar associations and open clusters in the Large Magellanic Cloud by Gouliermis et al. (2000), who also give a detailed description of the method.

The high resolution of ACS/WFC imaging and the large stellar sample allow the construction of detailed maps of the spatial density distributions for each stellar group (isodensity contour maps). The constructed contour maps are shown in Figure 4. The lowest isopleth corresponds to the background surface density and isopleths of higher surface density are plotted in steps of 1σ , where σ is the standard deviation of the background density. Any stellar concentration with density equal to or higher than 3σ above the background density (fourth isopleth in the maps of Figure 4) is consid-

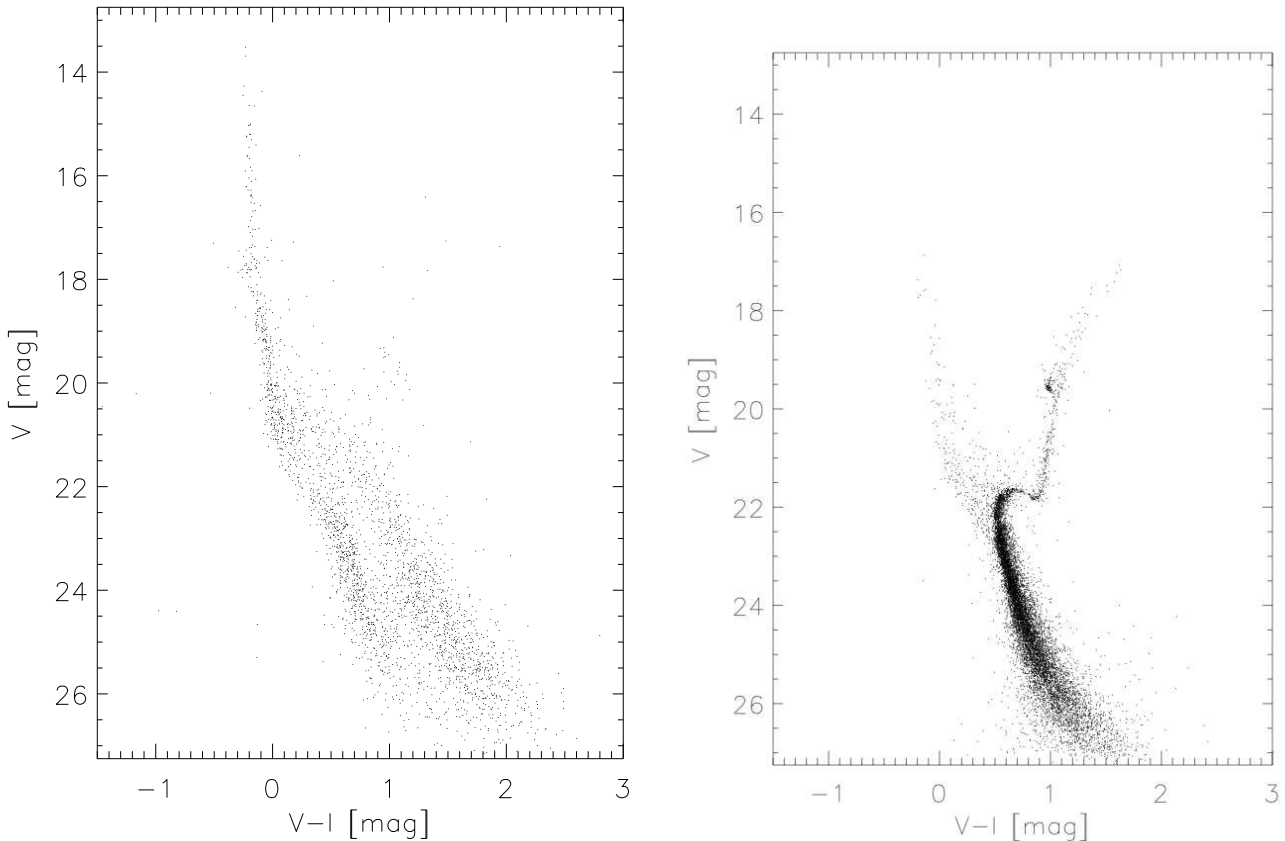


FIG. 5.— The $V-I$, V CMDs of the stars from our catalog confined within a boxed 14.1×10.2 pc area centered on the main body of the stellar association NGC 346 (left panel) and a circular area of radius 8.5 pc centered on the old star cluster BS 90 (right panel). The comparison of these CMDs exhibits the differences in stellar content of two stellar systems coexisting in the same region at a projected distance not larger than 24 pc from each other.

ered to be statistically significant. These maps show that not only different stellar populations dominate different areas of the observed region, but also their spatial distribution is very clumpy. The RGB and LMS groups seem to characterize mostly the massive old star cluster BS 90 (Bica & Schmitt 1995), while the UMS and PMS stars are mostly concentrated in the general area of the association NGC 346. It is interesting to note that two compact concentrations of UMS and PMS stars can be seen in the corresponding maps to the north-east of the main association.

4. THE DOMINANT STELLAR CONCENTRATIONS

The two dominant stellar systems in the area can be identified in the contour maps of Figure 4, from which an indication of the extent of the systems can be easily derived. Specifically, we select the areas, centered on the association NGC 346 and the cluster BS 90, as they are defined by the 3σ isopleths in Figure 4. For BS 90 we use the RGB and LMS maps and for the association the UMS and PMS ones. A circular area has been selected for the cluster, which has almost the same dimensions in both LMS and RGB contour maps. For the association we select a quadrilateral area, which confines the 3σ isopleth in both PMS and UMS contour maps. This kind of selection is made because of the irregular, non-spherical shape of the association, as it is typical for associations, which are characterized by their extended form. The location of the star cluster BS 90 is well defined by a circular area with radius around 8.5 pc, and the one of the main body of the associa-

tion NGC 346 by a box of dimensions 14.1×10.2 pc.

Obviously the majority of the stars confined in each of the selected regions belongs to the populations of the corresponding systems and hence they represent the main stellar content of the systems. Consequently the CMDs of the stars in each region correspond to each of the systems. These CMDs plotted for stars in the quadrilateral area centered on NGC 346 and a circle centered on BS 90 are both shown in Figure 5. These plots provide a first order distinction between the two dominant stellar concentrations in the star forming region of NGC 346/N 66, based on their stellar content. Consequently, these CMDs exhibit the variety of stellar species that are included in the relatively small observed $5' \times 5'$ region. Although BS 90 is a very bound and obviously massive star cluster (see map of Figure 1) it was never given much attention because of the fact that its stellar content does not include any blue massive stars, which were the main targets of previous works, and probably also because it was out-shined by the large number of bright blue super-giants of the association (see introduction).

Naturally, each of the CMDs shown in Figure 5 does not fully account only for the stellar population in each of the corresponding systems, because it is contaminated by the contribution not only of the general field of SMC at this region, which deserves an equally thorough study, but also of the population of the other system. This is more obvious in the CMD of BS 90 (right panel), where the upper main sequence is populated by a small number of blue giants up to $V \simeq 17$ mag.

Probably this contamination comes from the association NGC 346 itself. The CMD of BS 90 is extremely sharp with a very clear turn-off and red giants branch, that make it a template cluster for the study of old clustered populations in the low-metallicity SMC. A more detailed study on this cluster and its environment is under way for the investigation of the fundamental properties of the stellar content and the dynamical behavior of this cluster (Rochau et al. in preparation).

On the other hand the CMD of the area centered on NGC 346 association seems to be more clear from any old population contamination. A very interesting feature of this CMD is the very sharp upper main sequence, which is easily fitted by the ZAMS, making the age determination of the association from these data alone very difficult. Another interesting feature in this CMD is the secondary faint red sequence almost parallel to the lower main sequence, which obviously corresponds to the PMS population of the association in agreement with the findings of Nota et al. (2006). Furthermore, the higher detection limit in comparison to BS 90 is a clear indication of the higher extinction that takes place in the area of the association. The case of the association NGC 346 is currently under detailed study by us for the specification of the extent of this system, the contamination of its CMD from the general field and the determination of its massive and low-mass Initial Mass Function (Hennekemper et al. in preparation).

5. FINAL REMARKS

We take advantage of the large improvement in sensitivity and wide-field resolution provided by ACS to perform a detailed photometric study of the most active star forming region in the SMC. We use the ACS module of the photometric package DOLPHOT, which is especially designed for imaging with the ACS and we provide the full photometric catalog of all stars detected with short and long exposures in three ACS/WFC fields, that covers a region of about $5' \times 5'$ centered on the young stellar association NGC 346. This region is a typical example of mixed stellar populations in the low-metallicity environment of the SMC. The detailed study of the stellar systems and the ambient general field of SMC in the region will provide new constraints for the determination of fundamental properties of concentrated stellar populations, such as relaxation time-scales and their Mass Functions.

We distinguish on the observed CMD of almost 100,000 detected stars in total, four regions, as the most representative of

different varieties: Upper Main Sequence (UMS), Red Giant Branch (RGB), Lower Main Sequence (LMS) and Pre-Main Sequence (PMS) stars. We find that UMS and PMS represent mostly one of the two dominant stellar concentrations in the observed region, the stellar association NGC 346, while RGB and LMS are mostly populated at the recently discovered old star cluster BS 90 (Bica & Schmitt 1995). The CMDs of the stars confined in the main central part of each of these two systems exhibit their differences in terms of their stellar content: The association NGC 346 is a well extended star forming system, while the cluster BS 90 is an old massive spherical star cluster, which can be considered a template for old low-metallicity populations.

Two investigations, one on BS 90 (Rochau et al. in preparation) and the other on the association NGC 346 (Hennekemper et al. in preparation) are under way to throw more light on these completely different neighboring stellar concentrations in the SMC. These systems are only a part of the variety of interesting objects, that are located in the observed region. Such are the components of the HII region N 66 (Henize 1956), as they are distinguished by Davies et al. (1976), small young star clusters (Oey et al. 2004), and CO clouds (Rubio et al. 2000). In addition, the region is characterized by a plethora of X-ray sources (Nazé et al. 2003), emission stars and small nebulae (Meyssonnier & Azzopardi 1993), and radio sources (Loiseau et al. 1987; Filipovic et al. 2002), as well as luminous IR sources, revealed with ISO and IRAS (Wilke et al. 2003) and *Spitzer* (Brandl, 2005). Therefore we make the stellar catalog resulted from our photometry available, so that the whole astronomical community can benefit from these extremely useful and accurate data.

D. Gouliermis acknowledges the support of the German Research Foundation (Deutsche Forschungsgemeinschaft - DFG) through the individual grant 1659/1-1. This paper is based on observations made with the NASA/ESA Hubble Space Telescope, obtained from the data archive at the Space Telescope Science Institute. STScI is operated by the Association of Universities for Research in Astronomy, Inc. under NASA contract NAS 5-26555. This research has made use of NASA's Astrophysics Data System, *Aladin* (Bonnarel et al. 2000), *WCSTools* (Mink 2001), and the SIMBAD database, operated at CDS, Strasbourg, France.

REFERENCES

- Bica, E. L. D., & Schmitt, H. R. 1995, *ApJS*, 101, 41
 Bonnarel, F., et al. 2000, *A&AS*, 143, 33
 Bouret, J.-C., et al. 2003, *ApJ*, 595, 1182
 Brandl, B. R., et al. 2005, IAU Symposium, 227, "Massive star birth: A crossroads of Astrophysics", Eds. Cesaroni, R. et al. Cambridge: Cambridge University Press, p.311
 Brandner, W., Grebel, E. K., Zinnecker, H., & Brandl, B. 1999, IAU Symp. 190: New Views of the Magellanic Clouds, 190, 366
 Bjorkman J.E., & Cassinelli J.P., 1993, *ApJ* 409, 429
 Danforth, C. W., Sankrit, R., Blair, W. P., Howk, J. C., & Chu, Y.-H. 2003, *ApJ*, 586, 117
 Davies, R. D., Elliott, K. H., & Meaburn, J. 1976, *MmRAS*, 81, 89
 Dolphin, A. E., et al. 2001, *ApJ*, 562, 303
 Ferland, G. J., Korista, K. T., Verner, D. A., Ferguson, J. W., Kingdon, J. B., & Verner, E. M. 1998, *PASP*, 110, 761
 Filipovic M.D., et al. 2002, *MNRAS*, 335, 1085
 Gouliermis, D., Kontizas, M., Korakitis, R., Morgan, D. H., Kontizas, E., & Dapergolas, A. 2000, *AJ*, 119, 1737
 Gouliermis, D., Brandner, W., & Henning, T. 2006, *ApJL*, 636, L133
 Henize, K. G. 1956, *ApJS*, 2, 315
 Keller, S. C., Wood, P. R., & Bessell, M. S. 1999, *A&AS*, 134, 489
 Kennicutt, R. C. 1984, *ApJ*, 287, 116
 Koekemoer, A. M., Fruchter, A. S., Hook, R. N., & Hack, W. 2002, The 2002 HST Calibration Workshop : Hubble after the Installation of the ACS and the NICMOS Cooling System. Baltimore, MD: Space Telescope Science Institute, 337
 Koenigsberger, G., Kurucz, R. L., & Georgiev, L. 2002, *ApJ*, 581, 598
 Kudritzki, R. P. 2002, *ApJ*, 577, 389
 Loiseau N., Klein U., Greybe A., Wielebinski R., Haynes R.F. 1987, *A&A*, 178, 62
 Massey P., Parker J. W., & Garmany C. D. 1989, *AJ*, 98, 1305
 Massey, P., Puls, J., Pauldrach, A. W. A., Bresolin, F., Kudritzki, R. P., & Simon, T. 2005, *ApJ*, 627, 477
 Meyssonnier N., Azzopardi M. 1993, *A&AS*, 102, 451
 Mink, D. J. 2002, ASP Conf. Ser. 281: Astronomical Data Analysis Software and Systems XI, 281, 169
 Nazé, Y., et al. 2003, *ApJ*, 586, 983
 Nota, A., et al. 2006, *ApJL*, 640, L29
 Oey M. S., King N. L., & Parker J. W. 2004, *AJ*, 127, 163
 Peimbert, M., Peimbert, A., & Ruiz, M. T. 2000, *ApJ*, 541, 688
 Relaño, M., Peimbert, M., & Beckman, J. 2002, *ApJ*, 564, 704
 Rubio, M., et al. 2000, *A&A*, 359, 1139
 Sher, D. 1964, *The Observatory*, 84, 32
 Sirianni, M., et al. 2005, *PASP*, 117, 1049

Vink, J. S. 2001, *A&A*, 369, 574

Walborn, N. R., et al. 2000, *PASP*, 112, 1243

Wilke K., Stickel M., Haas M., Herbstmeier U., Klaas U., & Lemke D. 2003,
A&A, 401, 873

Ye, T., Turtle, A. J., & Kennicutt, R. C., Jr. 1991, *MNRAS*, 249, 722